

Microstructures and Mechanical Properties of Electron Beam-Welded Titanium-Steel Joints with Vanadium, Nickel, Copper and Silver Filler Metals

Ting Wang, Binggang Zhang, Houqin Wang, and Jicai Feng

(Submitted March 4, 2013; in revised form May 23, 2013; published online February 22, 2014)

Electron beam welding experiments of titanium alloy to stainless steel with V, Ni, Cu and Ag filler metals were carried out. The interfacial microstructures of the joints were examined by optical microscopy, scanning electron microscopy, and x-ray diffraction analysis. Mechanical properties of the joints were evaluated according to tensile strength and microhardness. The results showed that all the filler metals were helpful to restrain the Ti-Fe intermetallics formed in the Ti/Fe joint. The welds with different filler metals were all characterized by solid solution and interfacial intermetallics. And the type of solid solution and interfacial intermetallics were depended on the metallurgical reactions between the filler metals and base metals. The interfacial intermetallics were $\text{Fe}_2\text{Ti} + \text{Ni}_3\text{Ti} + \text{NiTi}_2$, TiFe , Ti_2Ag , and $\text{Cu}_2\text{Ti} + \text{CuTi} + \text{CuTi}_2$ in the joints welded with Ni, V, Ag, and Cu filler metals, respectively. The tensile strengths of the joints were primarily determined by the hardness of the interfacial intermetallics. The highest tensile strength was obtained in the joint welded with silver filler metal, which is about 310 MPa.

Keywords electron beam welding, mechanical properties, microstructure, stainless steel, titanium alloy

1. Introduction

Titanium alloys are preferred structural materials in the aeronautics and astronautics industries because of their high specific strength (Ref 1, 2). Stainless steels are widely used, inexpensive materials in most industrial fields (Ref 3). Therefore, there are urgent needs to join titanium and stainless steel, so that these alloys can be applied to reduce the weight and cost of various components.

It has been acknowledged that traditional fusion welding methods are not feasible for joining titanium alloys to stainless steels because of metallurgical incompatibilities. Therefore, solid-state joining method is a viable solution to overcome this difficulty by preventing the diffusions of alloying elements (Ref 4). However, direct solid-state joining is also very difficult attributed to the low solubility of iron in alpha titanium at room temperature. Kundu et al. (Ref 5) and Orhan et al. (Ref 6) suggested that the brittleness of Fe-Ti and Fe-Cr-Ti intermetallics compromised the mechanical properties of diffusion bonds between Titanium alloys and stainless steels. Dey et al. (Ref 7), Najafabadi et al. (Ref 8), and Mousavi and Sartangi

(Ref 9) proved that Ti-Fe intermetallics also formed in the Ti/Fe interfaces during friction welding and explosion welding of titanium alloys to stainless steels. Fracture mainly occurred at the intermetallic-based interface and the strength decreased with thickening of the intermetallic layer. Aleman et al. (Ref 10) reported the factor for crack formation during diffusion bonding of titanium alloys to stainless steels. That was a large internal stress induced by differences in linear expansion and thermal conductivity between titanium and steel. Currently, indirect joining is generally realized by adding an intermediate metal layer such as Ni, Al, Ag, or Cu to prevent atomic diffusion between Ti and Fe, Cr, or Ni (Ref 11-14). Of all the interlayer metals above, copper is adopted more frequently. Copper does not produce brittle intermetallics with iron, chromium, nickel, or carbon. Moreover, it is a soft metal which can relax the internal stress through inner deformation.

In the above literature, copper as well as other metals was used as interlayer during diffusion bonding. However, the process was time consumable to implement. Particularly, the components with complex geometric shapes could not be joined by diffusion bonding as well as other solid-state bonding methods due to the limitation of the joint shape. Additionally, components must be heated to elevated temperature during the diffusion bonding process, which is not recommended for some metals. Consequently, a feasible fusion welding method to join these two dissimilar metals is necessary for further development. As a non-contact fusion joining technique with high efficiency and flexibility, laser welding of titanium to steel with Mg interlayer was considered, but $\text{Mg}_{17}\text{Al}_{12}$ would form and lower the strength of the joint (Ref 15). Electron beam welding is considered to be the most frequently used fusion welding technique for joining dissimilar metals because of certain advantages such as high energy density, vacuum atmosphere, and precise control of heating position and area (Ref 16). Moreover, a very narrow heat affected zone can be produced.

Ting Wang, Binggang Zhang, and Jicai Feng, Shandong Provincial Key Laboratory of Special Welding Technology, Harbin Institute of Technology at Weihai, 2 Wenhua West Road, Weihai 264209, China; and **Houqin Wang**, State Key Laboratory of Advanced Welding and Joining, Harbin Institute of Technology, 92 Xidazhi Street, Harbin 150001, China. Contact e-mails: fgwangting@163.com and zhang_bg@126.com.

Zhang et al. (Ref 17) joined Ti₃Al and TC₄ titanium alloys by electron beam welding. The tensile strength of the joint reached 92% of that of the base metal. Jonghyun and Kawamura (Ref 18) investigated the electron beam welding of Zr-based BMG to Ni metal. The bending strength of the welded joint was higher than the yield strength of the Ni metal. Therefore, it is

reasonable to consider electron beam welding as a preferred candidate process for the fusion welding of titanium alloys to stainless steels.

As with diffusion bonding, filler metal is also required for electron beam welding. In this paper, near α -type Ti6Al2Mo2V2Zr alloy and 304 type stainless steel (18Cr9Ni) were electron beam-welded with different filler metals, such as Ni, V, Cu, and Ag. The metallurgical processes of Ti and Fe elements with different filler metals were discussed by microstructure analysis. The feasibilities of the filler metals for joining titanium alloy to stainless steel were compared by mechanical property testing. Finally, a selecting law of the filler metal for electron beam welding of titanium alloy to stainless steel was concluded.

Table 1 Physical properties of the base metals at room temperature

Alloy type	Melting point, °C	Specific heat, J/kg/K	Thermal conductivity, W/m/K	Linear expansion coefficient, 10 ⁻⁶ /K
Ti-6-2-2-2	1677	495	7.4	8.6
304	1450	461	14.6	16.0

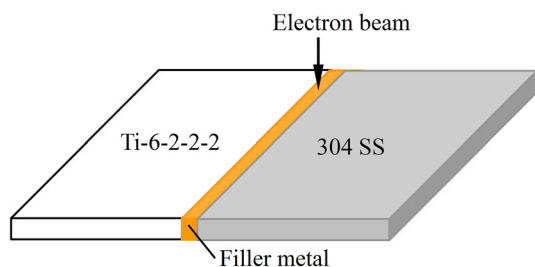


Fig. 1 Schematic diagram of the welding procedure

2. Experimental Procedures

2.1 Materials and Preparation

The materials used in the experiments were a near α -type titanium alloy (Ti6Al2Mo2V2Zr) and 304 austenitic stainless steel (18Cr9Ni). Physical properties of the alloys are given in Table 1.

In Table 1, large differences in the thermal conductivity and the linear expansion coefficient between the two base metals can be found. These will lead large temperature gradients and thermal stresses in the joint during the welding process (Ref 19). The metals were machined into 50 mm × 25 mm × 2.5 mm plates and then mechanically and chemically cleaned

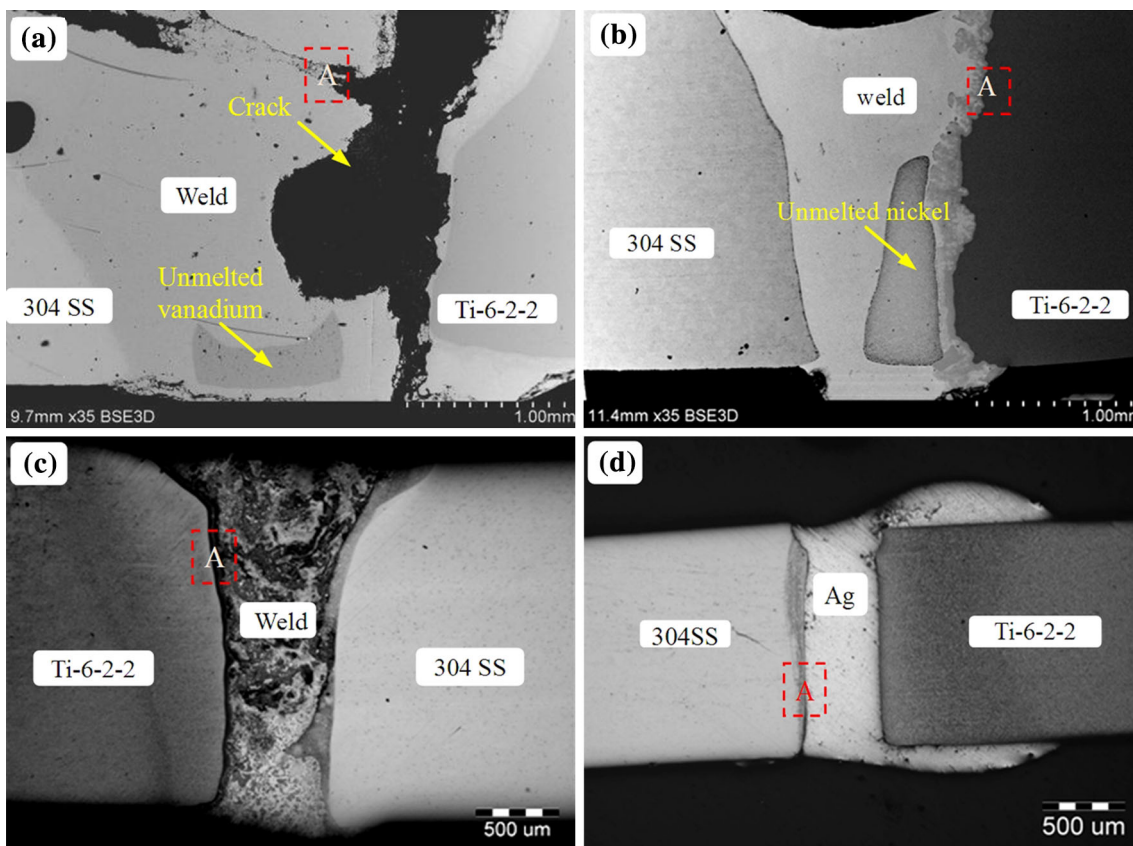


Fig. 2 Macrostructures of the cross sections of the EBW joints with different filler metals (a—vanadium, b—nickel, c—copper, d—silver)

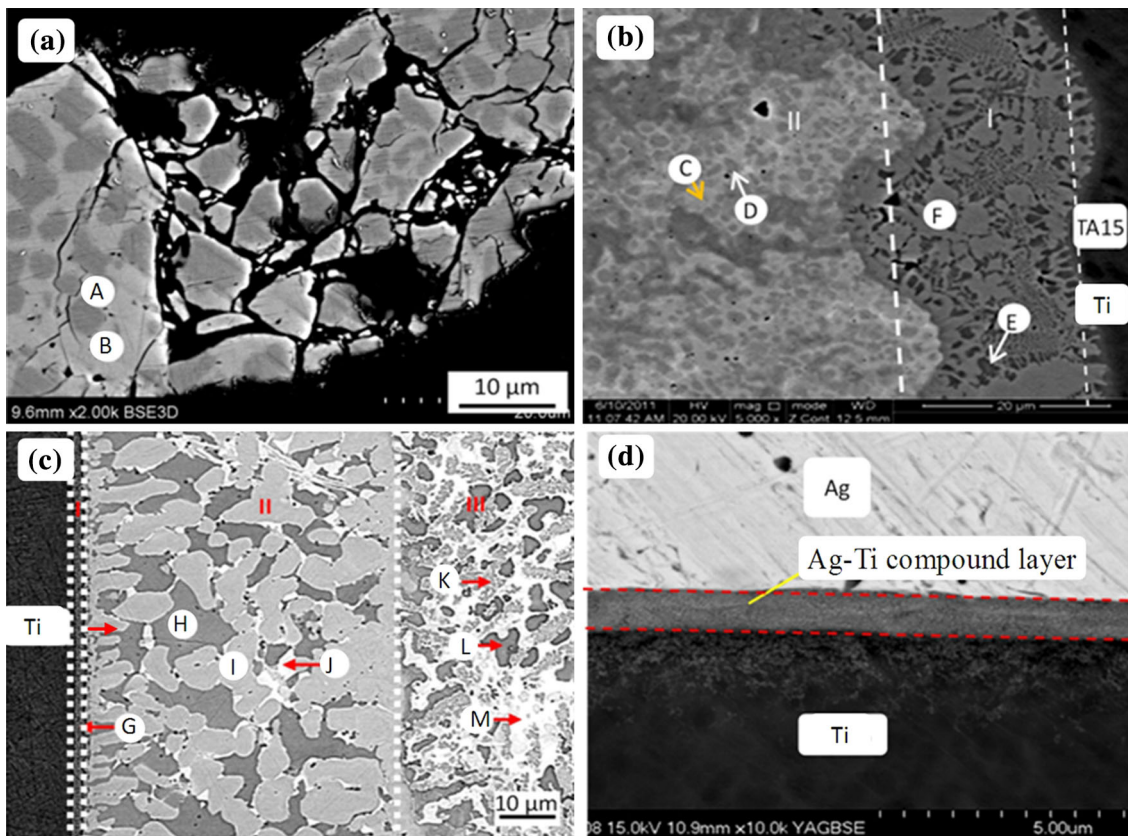


Fig. 3 Microstructures at the Ti side interfaces of the Ti/steel joints with different filler metals (a—vanadium, b—nickel, c—copper, d—silver)

before welding. 0.5 mm thick commercial pure vanadium, nickel, copper, and silver sheets were used as filler metals and were embedded in the contact faces before welding as Barreda et al. (Ref 20) and Irisarri et al. (Ref 21) did in their researches.

2.2 Welding Process and Test Work

Electron beams were focused on the centerlines of the filler metal sheets with the following parameters: accelerating voltage of 55 kV, focus current of 2450 mA, welding speed of 6 mm/s, and beam current of 9–12 mA. A schematic diagram of the welding procedure is shown in Fig. 1.

Specimens for microstructure characterization and hardness examination were prepared metallographically and then etched in a reagent of 20 mL HNO₃, 20 mL HF, and 80 mL H₂O. Microstructure observations on cross sections of the joints were carried out by optical and scanning electron microscopy. The elemental composition was evaluated by SEM-EDS in spot mode. X-ray diffraction analysis was carried out to identify the intermetallics. The operating voltage was 50 kV and the current was 25 mA using a Cu target. The scanning range was 20°–100° (2θ) at a speed of 3°/min. Vicker's microhardness was measured using a load of 100 g. Tensile testing was performed to evaluate the joint strength. The specimens were machined into rectangular bars (50 mm × 5 mm × 2.5 mm). The tests were carried out at room temperature and the displacement speed was 0.5 mm/min. Five samples were prepared for measurements of hardness and tensile strength for each condition.

3. Results and Discussion

3.1 Microstructures of the Joint Cross Sections

3.1.1 Macrostructures of the Cross Sections. Figure 2 shows the cross-section macrostructures of the electron beam-welded Ti/steel joints with different filler metals. Sound joint could not be achieved with V filler metal due to the through crack propagation at the interface between Ti alloy and the weld. Low melting point Ag filler metal melted completely while partial V and Ni filler metals residual in the welds because of their high melting points. The base metals did not melt along with the Ag filler metal, and thus enabling an electron beam brazing process.

3.1.2 Microstructures of the Ti Side Interfaces. Ti is an active element and tends to form intermetallics with multiple metal elements. Hence, the microstructure of the Ti side interface was analyzed and comparatively studied. The microstructures at the Ti side interfaces of the Ti/steel joints are shown in Fig. 3. Constituent phases of the interfaces were analyzed combined with EDS analysis (Table 2).

Dense cracks formed around the through crack in the Ti side interface constituted by dispersive blocky phase A and continuous network phase B when V filler metal was selected. As the Ti-Fe-V ternary phase diagram (seen in Fig. 4) shows that there was no ternary intermetallic compound between the three elements (Ref 22). The solid solubility of V in TiFe was

Table 2 Chemical compositions of the different phases (at.%) in the interfaces

	Ti	Fe	Cu	Cr	V	Ni	Potential phases
A	25	25	0	9	40	1	TiFe
B	38	37	0	4	22	4	TiFe
C	26	27	0	7	0	40	Fe ₂ Ti + Ni ₃ Ti
D	24	21	0	7	0	48	Fe ₂ Ti + Ni ₃ Ti
E	73	8	0	4	0	15	α-Ti
F	60	7	0	4	0	29	NiTi ₂
G	76	5	15	0	0	4	Ti + Ti ₂ Cu
H	60	2	28	7	0	3	Ti ₂ Cu
I	44	6	45	2	0	2	TiCu
G	34	1	60	0	0	5	TiCu ₂
K	46	21	26	4	0	3	τ ₃
L	4	2	88	3	0	2	Copper
M	36	13	42	6	0	3	τ ₂

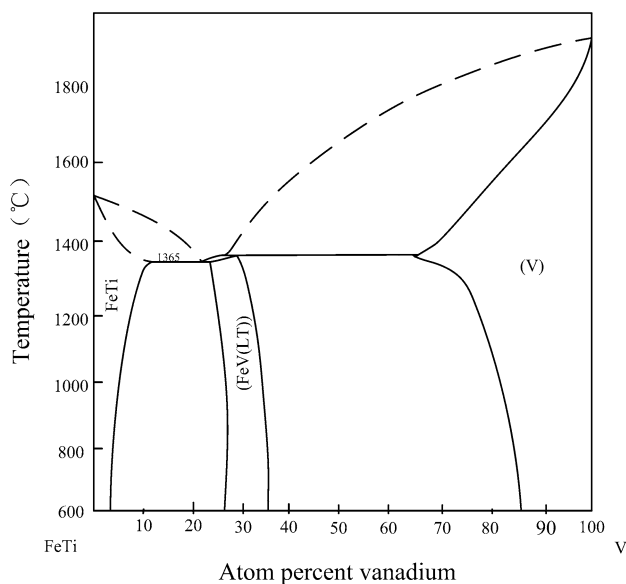


Fig. 4 TiFe-V ternary phase diagram

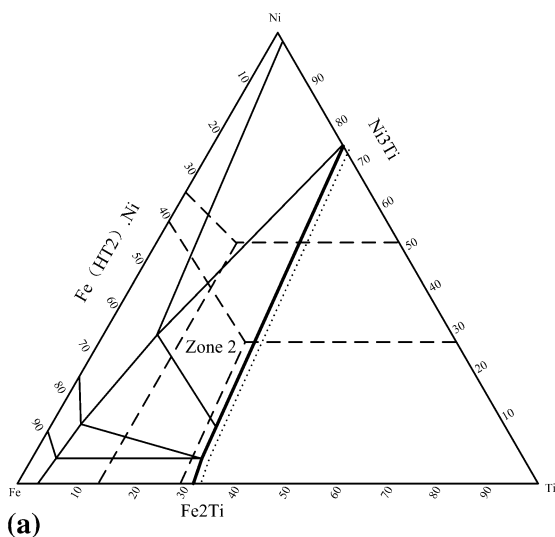


Fig. 5 (a) Ti-Fe-Ni ternary phase diagram and (b) Ti side of Ti-Ni binary phase diagram

rather low. Combined with the EDS results, we can anticipate that phase A and phase B were TiFe phase with different supersaturated V element content which was formed during the rapid cooling process of electron beam welding.

The Ti side weld with Ni filler meta can be divided into two morphologically distinct zones, which were denoted by zone I and zone II. Combined with Ti-Ni-Fe ternary phase diagram (seen in Fig. 5a) (Ref 23) and Ni-Ti binary phase diagram (seen in Fig. 5b) (Ref 24), zone II, which was located in the triple-phase region, was a mixture of (α-Fe, Ni) solid solution, Fe₂Ti (Phase C), and Ni₃Ti (Phase D). Zone I was mainly composed of Ni₂Ti (Phase F), with a small amount α-Ti (Phase E) dispersed around it. Figure 6(a) shows the phases were confirmed by XRD analysis.

Microstructure in Ti side weld with Cu filler metal is given in Fig. 3(b). This region is divided into three zones according to their morphology characteristics, and they are marked as zone I, II, and III, respectively. From the EDS results as well as Ti-Cu (Ref 25) and Ti-Cu-Fe (Ref 23) phase diagrams (seen in Fig. 7), zone I consists of solid solution of titanium with some Ti₂Cu (phase G) in it. Zone II is characterized by blocky compounds Ti₂Cu (phase H) and TiCu (phase I) as well as dispersedly distributed fine TiCu₂ (phase J). It needs to be noted that Cu₂Ti is a kind of metastable phase existing in the temperature range of 890-870 °C. But it was retained at room temperature in this joint for the high cooling rate during electron beam welding. Zone III contains three phases, i.e., dark gray blocky Ti₄₃Cu₅₇-Fex (x = 21-24) denoted as τ₃ (phase K), with the same lattice type as Cu₄Ti₃, light gray phase Ti₄₀Cu₆₀-xFex (x = 5-17) denoted as τ₂ (phase M), with the same lattice type as Cu₃Ti₂ and solid solution of copper (phase L). The above anticipated phases were confirmed by XRD analysis (Fig. 6b).

The joint with Ag filler metal showed a typical braze characteristics. An obvious interface layer generated between the braze and Ti base metal. It can be inferred that the interfacial compound was Ti₂Ag by the EDS results and Ti-Ag binary phase diagram (seen in Fig. 8) (Ref 26). The interface layer was generated by diffusion of the liquid Ag atoms into solid Ti base metal. The thickness of the interface layer was only about 1 μm, which was related to the rapid heating and cooling rate characteristic of the electron beam welding.

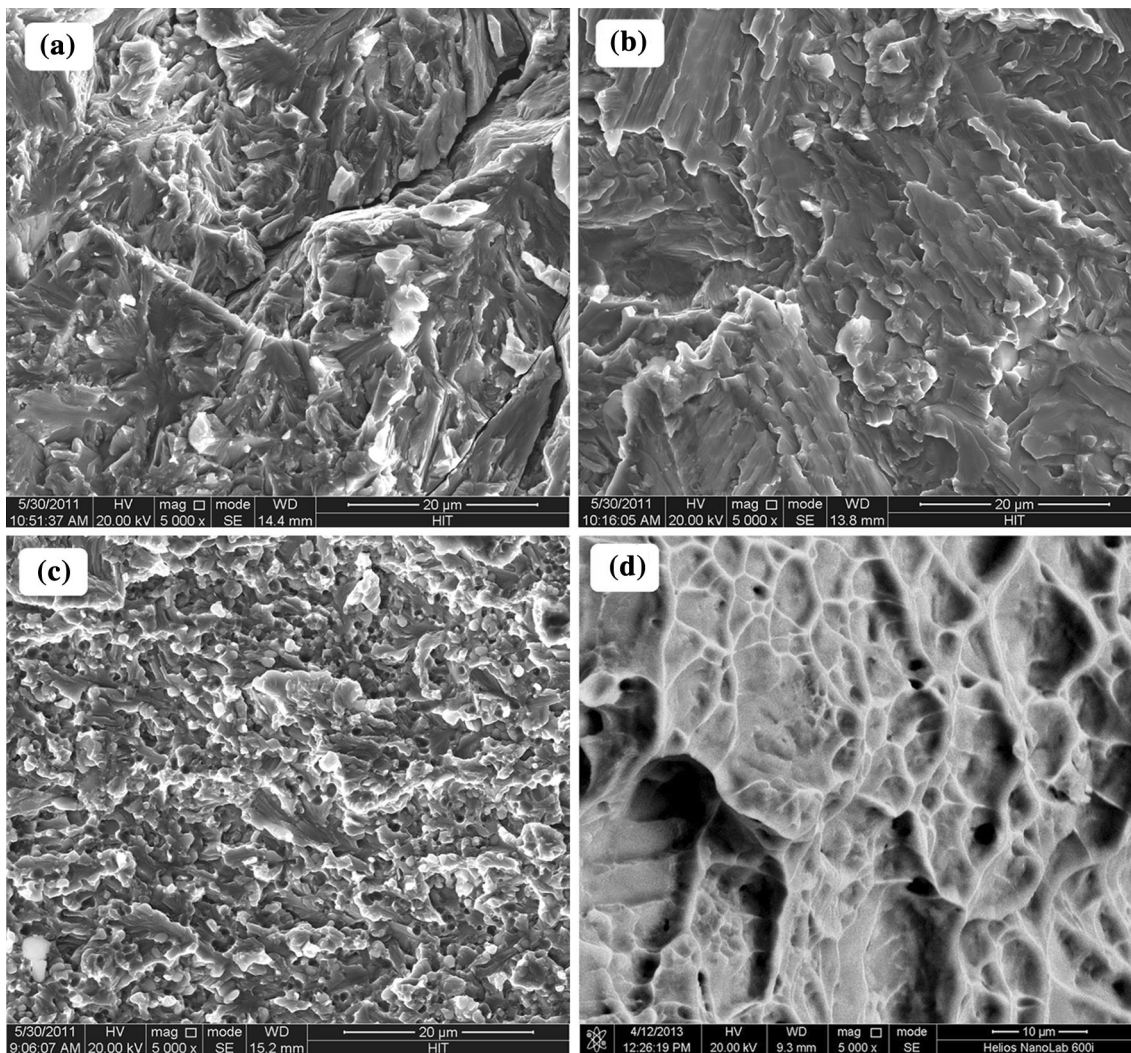


Fig. 9 Fracture surface morphologies of the joints with different filler metals (a—vanadium, b—nickel, c—copper, d—silver)

also cracked in Ti-Cu and Ti-Ni compound layers during tensile test. It is clear that the brittle compound layers are the weakest parts in the joints. The fracture surfaces are given in Fig. 9. The surface morphologies of Ti/V/Fe and Ti/Ni/Fe joints show brittle cleavage fracture mode for the high brittleness of the compound layers. Secondary cracks can also be observed in these fracture surfaces, which lead bad joining strength. For the Ti/Cu/Fe joint, hardness of the compound layer (~580 HV) was lower than that of Ti/Ni/Fe joint. A quasi-cleavage fracture mode was obtained according to the fracture surface morphology. As a result, the tensile strength increased significantly. However, the Ti/Ag/Fe joint cracked in Ag filler metal because of the relatively soft (~204 HV) and very thin (~1 μm) compound layer. The fractograph demonstrated a dimple pattern with features of plastic fracture. Consequently, the highest tensile strength was achieved.

4. Conclusion

(1) The joint strength with V filler metal was the poorest with through crack at the Ti side interface zone, while sound joint was achieved with Ni and Cu filler metal, respec-

tively. The joint with Ag filler metal shows the typical braze characteristics. The interfacial intermetallics were $\text{Fe}_2\text{Ti} + \text{Ni}_3\text{Ti} + \text{NiTi}_2$, TiFe , Ti_2Ag , and $\text{Cu}_2\text{Ti} + \text{CuTi} + \text{CuTi}_2$ in the joints welded with Ni, V, Ag, and Cu filler metals, respectively.

- (2) The tensile strengths of the joints were primarily determined by the thickness and brittleness of the interfacial intermetallics. The microhardness value order of the joint was V, Ni, Cu, and Ag, from high to low order, while the tensile strength order of the joint was opposite. Of all, the highest tensile strength was obtained in the joint welded with silver filler metal, which is about 310 MPa.
- (3) The tensile strength was related to average hardness of the interface compound layer. The joint with good toughness was benefit to the elevation of the joint strength. The joints with high hardness compound layers showed brittle cleavage fracture mode and quasi-cleavage or dimple plastic fracture modes were detected in the joints with relatively soft interfacial compounds.
- (4) The feasibilities of the filler metals for electron beam welding of titanium alloy to stainless steel were primarily based on the toughnesses of the products and the difficulty levels of the metallurgical reactions among the elements in filler metals and base metals.

Acknowledgments

This work was supported by Natural Scientific Research Innovation Foundation in Harbin Institute of Technology (HIT.NS RIF.2014130) and International Science & Technology Cooperation Program of China (2011DFR50760).

References

1. R.R. Boyer, An Overview on the Use of Titanium in the Aerospace Industry, *Mater. Sci. Eng. A*, 1996, **213**, p 103–114
2. E.O. Ezugwu and Z.M. Wang, Titanium Alloys and Their Machinability: A Review, *J. Mater. Process. Technol.*, 1997, **68**, p 262–274
3. J.L. Yang, Y. Li, and F. Wang, New Application of Stainless Steel, *J. Iron Steel Res. Int.*, 2006, **13**, p 62–66
4. C. Sudha, T.N. Prasanthi, S. Murugesan et al., Study of Interface and Base Metal Microstructures in Explosive Clad Joint of Ti-5Ta-1.8Nb and 304L Stainless Steel, *Sci. Technol. Weld. Join.*, 2011, **16**, p 133–139
5. S. Kundu, S. Sam, and S. Chatterjee, Interface Microstructure and Strength Properties of Ti-6Al-4V and Microduplex Stainless Steel Diffusion Bonded Joints, *Mater. Des.*, 2011, **32**, p 2997–3003
6. N. Orhan, T.I. Khan, and M. Eroglu, Diffusion Bonding of a Microduplex Stainless to Ti-6Al-4V, *Scripta Mater.*, 2001, **45**, p 441–446
7. H.C. Dey, M. Ashfaq, A.K. Bhaduri, and K.P. Rao, Joining of Titanium to 304L Stainless Steel by Friction Welding, *J. Mater. Process. Technol.*, 2009, **209**, p 5862–5870
8. M. Fazel-Najafabadi, S.F. Kashani-Bozorg, and A. Zarei-Hanzaki, Joining of CP-Ti to 304 Stainless Steel Using Friction Stir Welding Technique, *Mater. Des.*, 2010, **31**, p 4800–4807
9. S.A.A.A. Mousavi and P.F. Sartangi, Experimental Investigation of Explosive Welding of cp-Titanium/AISI, 304 Stainless Steel, *Mater. Des.*, 2009, **30**, p 459–468
10. B. Aleman, I. Gutierrez, and J.J. Urcola, Interface Microstructures in Diffusion Bonding of Titanium Alloys to Stainless and Low Alloy Steels, *Mater. Sci. Technol.*, 1993, **9**, p 633–641
11. S. Kundu and S. Chatterjee, Characterization of Diffusion Bonded Joint Between Titanium and 304 Stainless Steel Using a Ni Interlayer, *Mater. Charact.*, 2008, **59**, p 631–637
12. E. Atasoy and N. Kahraman, Diffusion Bonding of Commercially Pure Titanium to Low Carbon Steel Using a Silver Interlayer, *Mater. Charact.*, 2008, **59**, p 1481–1490
13. A. Elrefaey and W. Tillmann, Solid State Diffusion Bonding of Titanium to Steel Using a Copper Base Alloy as Interlayer, *J. Mater. Process. Technol.*, 2009, **209**, p 2746–2752
14. N. Özdemir and B. Bilgin, Interfacial Properties of Diffusion Bonded Ti-6Al-4V to AISI, 304 Stainless Steel by Inserting a Cu Interlayer, *Int. J. Adv. Manuf. Technol.*, 2009, **41**, p 519–526
15. M. Gao, S.W. Mei, and Z.M. Wang, Characterisation of Laser Welded Dissimilar Ti/Steel Joint Using Mg Interlayer, *Sci. Technol. Weld. Join.*, 2012, **17**, p 269–276
16. Z. Sun and R. Karppi, The Application of Electron Beam Welding for the Joining of Dissimilar Metals: An Overview, *J. Mater. Process. Technol.*, 1996, **59**, p 257–267
17. H.T. Zhang, P. He, J.C. Feng, and H.Q. Wu, Interfacial Microstructure and Strength of the Dissimilar Joint Ti₃Al/TC₄ Welded by the Electron Beam Process, *Mater. Sci. Eng. A*, 2006, **425**, p 255–259
18. J. Kim and Y. Kawamura, Electron Beam Welding of Zr-Based BMG/Ni Joints: Effect of Beam Irradiation Position on Mechanical and Microstructural Properties, *J. Mater. Process. Technol.*, 2008, **207**, p 112–117
19. Y.H. Wei, Z.B. Dong, and B. Liu, Stress Distributions of Welding Joints in Titanium-Steel Composite Pressure Vessel Under Working Conditions, *Sci. Technol. Weld. Join.*, 2011, **16**, p 709–716
20. J.L. Barreda, F. Santamaria, and X. Azpiroz, Electron Beam Welded High Thickness Ti6Al4V Plates Using Filler Metal of Similar and Different Composition to the Base Plate, *Vacuum*, 2001, **62**, p 143–150
21. A.M. Irisarri, J.L. Barreda, and X. Azpiroz, Influence of the Filler Metal on the Properties of Ti-6Al-4V Electron Beam Weldments. Part I: Welding Procedures and Microstructural Characterization, *Vacuum*, 2009, **84**, p 393–399
22. V. Raghavan, Fe-Ti-V(Iron-Titanium-Vanadium), *J. Phase Equilib.*, 1993, **14**(5), p 632
23. P. Villars, P. Alan, and O. Hiroaki, *Handbook of Ternary Alloy Phase Diagrams*, ASM International, Materials Park, OH, 1995
24. J.L. Murray, *Ni-Ti(nickel-titanium), Phase Diagrams of Binary Nickel Alloys*, ASM International, Materials Park, OH, 1991
25. J.L. Murray, The Cu-Ti(Copper-Titanium) System, *J. Phase Equilib.*, 1983, **4**(1), p 81–95
26. J.L. Murray and K.J. Bhansali, The Ag-Ti(Silver-Titanium) System, *J. Phase Equilib.*, 1983, **4**(2), p 178–183
27. W. Lu, Y. Shi, X. Li, and Y. Lei, Correlation Between Tensile Strength and Hardness of Electron Beam Welded TC4-DT Joints, *J. Mater. Eng. Perform.*, 2013, **22**, p 1694–1700
28. A. Elrefaey and W. Tillmann, Correlation Between Microstructure, Mechanical Properties, and Brazing Temperature of Steel to Titanium Joint, *J. Alloys Compd.*, 2009, **487**, p 639–645